KSCE Journal of Civil Engineering (2024) 28(4):1183-1193
DOI 10.1007/s12205-024-0588-4

pISSN 1226-7988, eISSN 1976-3808
www.springer.com/12205

Geotechnical Engineering

Pullout Behavior of Suction Piles in Saturated Sand Subjected to Combined Vertical and Horizontal Loading – Centrifuge and Finite Element Analysis

You-Seok Kim[a], **Youngseok Jo**[b], **and Yeon-Soo Jang**[c]

[a]*Member, Institute of Construction Technology, DAEWOO Engineering & Construction Co., Ltd., Suwon 04548, Korea*
[b]*Dept. of Civil and Environmental Engineering, University of California at Berkeley, Berkeley, CA 94709, USA*
[c]*Member, Geotechnical Institute, SAEGIL E&C CO. Ltd., Seoul 05854, Korea*

ARTICLE HISTORY

Received 29 March 2023
Revised 30 August 2023
Accepted 13 November 2023
Published Online 18 January 2024

KEYWORDS

Suction pile
Ultimate pullout capacity
Centrifugal model test
Finite element analysis
Failure envelope
Catenary and Taut-leg mooring systems

ABSTRACT

Suction piles have increasingly been considered as foundations for offshore facilities. In this study, the pullout behaviors of suction piles embedded in saturated sand subjected to combined vertical and horizontal loading at various inclination angles and pad-eye positions are investigated carrying out centrifugal tests and finite element (FE) analyses. The ultimate pullout capacities obtained from the model tests and FE analyses both increased as the inclination angle was close to 0° and the pad-eye position approached 75% of the pile length from the lid. This is associated with the increase of the passive earth pressure and friction between the soil and suction pile while the pile is pulled out. The failure envelopes were suggested depending on pad-eye positions to improve the design approach for offshore foundations. The optimal pad-eye positions for catenary and taut-leg mooring systems were then investigated by additional FE analyses to demonstrate the practical implications. For both mooring systems, the largest ultimate pullout capacity was obtained when the pad-eye was located at 75% of the suction pile length below the lid. The ultimate pullout capacity of the catenary mooring system was determined to be 1.94 times that of the taut-leg mooring system under the same conditions.

1. Introduction

Suction piles initially started in the 1970s, and they have been widely used since the 1980s as foundations for mooring offshore facilities, e.g., floating oil and gas exploration and extraction platforms, flowlines, and floating wind turbines (Andersen and Jostad, 1999; Aubeny et al., 2003; Randolph and House, 2002). The suction pile has a pad-eye on the lid or the side of the pile, and the offshore facilities are connected to the pad-eye through a mooring line to bear the up-lift or buoyant forces. The pullout capacity of the suction pile in this configuration is strongly dependent on the combined vertical and horizontal loading according to the pad-eye positions and inclination angles. Therefore, it is necessary to examine an appropriate mooring system with a high ultimate pullout capacity to ensure the safety of structures in coastal environments.

The pullout capacity of a suction pile is related to various factors (e.g., soil condition, pad-eye position, inclination angle, and aspect ratio). Therefore, many researchers have analyzed the pullout behavior of suction piles according to these various factors carrying out the centrifugal model tests (Bang et al., 2011; Gao et al., 2013; Kim et al., 2015; Koh et al., 2017; Ssenyondo et al., 2021) and the finite element analyses (Ahmed and Hawlader, 2015; Kim et al., 2016; Petel and Singh, 2019; Keawsawasvong et al., 2021). Note that the term "suction pile" has not yet been clearly defined and this pile is often referred to by various terms (e.g., suction caisson, suction bucket foundation, suction anchor, and skirted foundations) according to the specific application (Tjelta, 2001).

Bang et al. (2011) analyzed the effects of various inclination angles and pad-eye positions on the ultimate pullout capacity of the suction pile in sand by a series of centrifugal model tests and it was concluded that the optimal pad-eye positions are located between 70% and 75% of the pile height. Gao et al. (2013) performed centrifugal model tests to analyze the pullout behavior and optimal pad-eye positions of a suction caisson in clay. Based

CORRESPONDENCE Youngseok Jo ysjo_david@berkeley.edu Dept. of Civil and Environmental Engineering, University of California at Berkeley, Berkeley, CA 94709, USA

on the results, they stated that the optimal pad-eye position was between the top 2/3 and 3/4 of the caisson height. Kim et al. (2015) analyzed the performance of group suction anchors, installed in silty sand and subjected to horizontal pullout loading, using centrifugal model tests and numerical simulations. They concluded that the pullout capacity increased as the length of the anchor increased due to the increase in skin friction. Koh et al. (2017) analyzed the pullout behavior of a suction caisson anchor, embedded in Calcareous silt, with various inclination angles, performing a series of centrifugal model tests. It was reported that the pullout capacity increased as the inclination angle decreased. Ssenyondo et al. (2021) investigated the effect of embedment depth on the pullout capacity of suction bucket foundations embedded in sand, by conducting a series of 1 g experiments and concluded that the pullout capacity increased with the embedment depth.

Kim et al. (2016) carried out three-dimensional FE numerical analyses to calculate the horizontal ultimate pullout capacity of suction anchors, installed in silty sand, with various pad-eye positions. They concluded that the optimal pad-eye positions were located at 70% of the pile height. Ahmed and Hawlader (2015) carried out three-dimensional FE analyses to evaluate the pullout capacity of a suction caisson, embedded in dense sand, subjected to oblique loadings using the Abaqus FE software. They mentioned the following three conclusions; 1) the caisson's rotation significantly influenced the pullout capacity; 2) the failure wedge formed by the displacement of the caisson was a function of the inclination angle and pad-eye position; 3) the largest ultimate pullout capacity was obtained when the pad-eye was located at 75% of the pile length with an inclination angle of 0°. Peter and Singh (2019) conducted a parametric study on the vertical pullout capacity of a suction caisson in cohesive soil using a series of two-dimensional FE analyses. They reported that the pullout capacity increased as the soil cohesion, friction angle, and caisson length increased. Keawsawasvong et al. (2021) analyzed the effect of anisotropic undrained shear strengths of clays on the pullout capacity of suction caissons by performing the FE limit analysis and proposed design charts based on the relationship among the pullout capacity, undrained shear strength, and adhesion between the caisson and clay.

As described above, even though many studies related to the pullout capacities and behavior of suction piles have been conducted, most studies were focused on the pullout behavior of suction piles embedded in clayey soils, not sandy soils. In Korea, for renewable energy, studies have been performed, since the 2010s, regarding building offshore wind turbines. Recently, construction companies in Korea have begun planning to build them on the East Sea located on the right side of the Korean Peninsula. The suction piles have been considered a mooring system for floating offshore wind turbines, and the bottom of the East Sea consists of silty sand and sandy soil (Fig. S1). Therefore, in this study, a series of centrifugal model tests and finite element (FE) analyses were performed to investigate the pullout behavior of a suction pile embedded in saturated sand with inclination angles ranging from 0° to 90° and pad-eye positions ranging from 5% to 95% of the pile length below the lid. In particular, since no one has performed centrifugal model tests in conjunction with FE analyses so far in the world in order to analyze the pullout behavior of suction piles embedded in sandy soils, this study has described the pullout behavior of suction piles depending on the various inclination angles and pad-eye positions by analyzing the results of centrifugal model tests conjunction with FE analyses. Herein, a series of centrifugal model tests were motivated by the previous works of Bang et al. (2011) and Jang and Kim (2013). Based on the results, the optimal pad-eye position and inclination angle were then analyzed in which the largest ultimate pullout capacity subjected to combined vertical and horizontal loading can be generated. The vertical-horizontal (V-H) failure envelopes were subsequently suggested to develop the design method for offshore foundations in the coastal environment. In addition, the practical implications of the catenary and taut leg mooring systems were discussed.

2. Centrifugal Model Tests

2.1 Centrifuge Equipment

The centrifuge used in this test was, a C65-20, made by Actidyn, France. This machine has 3 m of arm and can accommodate a payload of up to 12 kN at the 100 g levels, which means 5.5 kN at the 200 g levels. As a beam type of centrifuge, it has a basket at the end of the arm, and a counterweight at the opposite side to balance a center of weight. The container used in this experiment is made of steel, with dimensions of 80 cm in length, 50 cm in height, and 20 cm in width. The transparent plexiglass 40 mm thick is attached in front of the container for internal observation (Fig. 1).

Figure 2 shows an overall view of the pulling systems mounted in the centrifuge container. The horizontal and inclined pullout capacities of the suction pile were respectively measured using equipment without (Fig. 2(a)) and with (Fig. 2(b)) the inclination angle controller. The pulling rate was set to 0.6 mm/sec which is a sufficiently slow speed to be able to consider the characteristics of very coarse sand used in this study (i.e., if the D_{50} of used sand is equal to 0.5 mm. In terms of the pulling rate, it did not affect

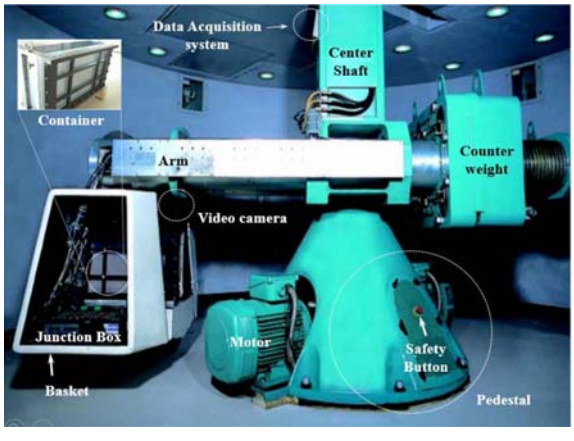

Fig. 1. The C65-20 Centrifuge Used in This Study

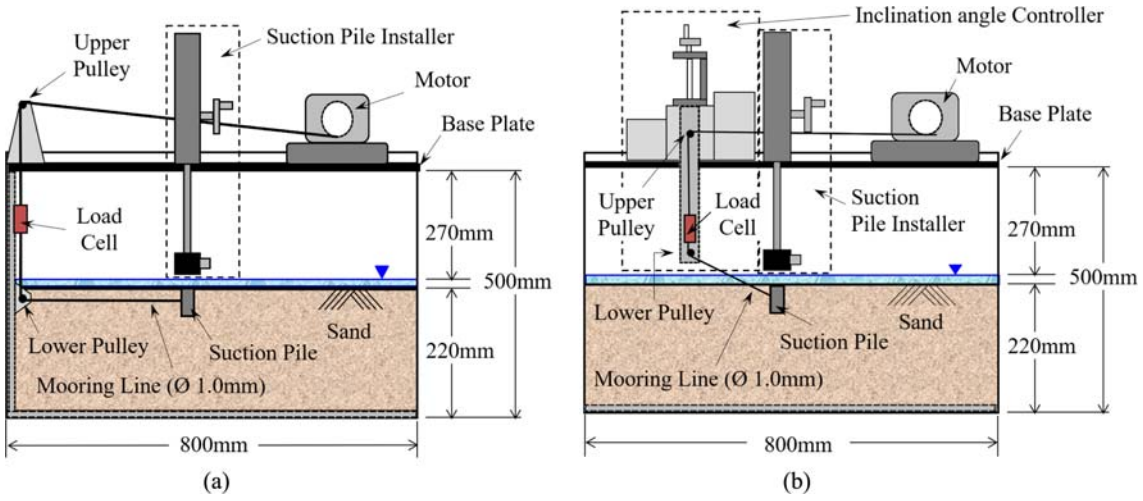

Fig. 2. Schematic Drawing of the Pulling System: (a) Without an Inclination Angle Controller to Measure Horizontal Pullout Capacity, (b) With an Inclination Angle Controller to Measure Inclined Pullout Capacity

Table 1. Specifications of the Model and Proto-Type Suction Piles

Shape	Pile Length, L_0		Outside Diameter, D		Thickness, t		g Level	Young's Modulus, E (GPa)
	Model (mm)	Proto-type (m)	Model (mm)	Proto-type (m)	Model (mm)	Proto-type (m)		
Hollow cylinder	60	6.0	30	3.0	1.0	0.1	100	200

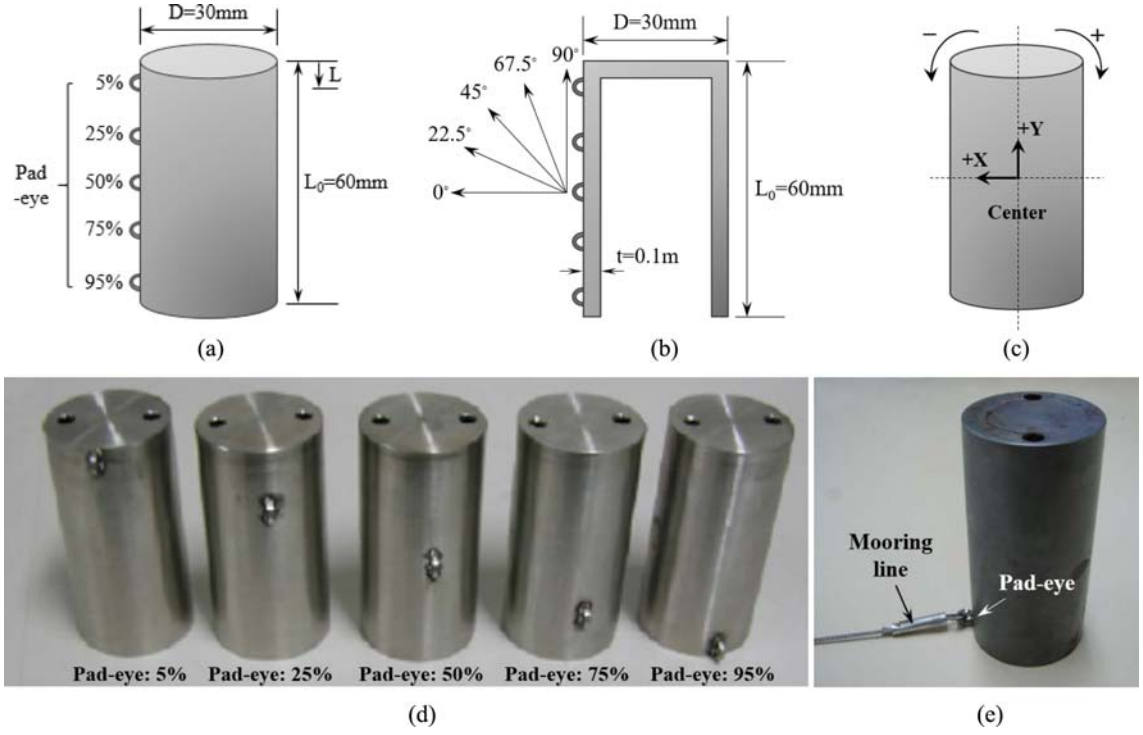

Fig. 3. Model Suction Piles For Centrifugal Model Tests Measuring Pullout Capacity: (a) Pad-Eye Positions (L/L_0), (b) Inclination Angles, (c) Sign Convention, (d) Completed Specimens Showing Pad-Eye Positions, (e) Mooring Line Connection to the Pad-Eye

the pullout capacities on the centrifugal model tests), even though the rate was reduced to 0.06 mm/sec. It implied that the pulling rate was sufficient and the drained condition of sandy soils was considered appropriate. A detailed description has been delineated in Kim (2014). The data describing the pullout capacities with suction pile displacement were collected four times per second.

2.2 Model Suction Pile

Five model suction piles were prepared for the centrifugal model tests. These suction piles have the length (L_0), outside diameter (D), and thickness (t) of 60 mm, 30 mm, and 1 mm, respectively, corresponding to an aspect ratio (L_0/D) of 2.0. The centrifugal model tests were carried out at the 100g level as the models represented 1:100 scale proto-types. The specifications of the model and proto-type suction piles are shown in Table 1.

Figure 3 shows the model specimens used in the tests. The pad-eye was attached to one of five different positions on each specimen, i.e., 5%, 25%, 50%, 75%, and 95% of the pile length below the lid. In which, the pad-eye position (L/L_0) is defined as the ratio of the distance between the lid and the pad-eye position (L) to the total length of the pile (L_0) (Fig. 3(a)). For each pad-eye position, the suction pile was pulled out during the centrifugal model tests according to the applied inclination angle, which was set to 0.0°, 22.5°, 45.0°, 67.5°, or 90.0° (Fig. 3(b)). The sign convention used to describe the results of the model tests is defined in Fig. 3(c). The model suction piles were pulled out at the desired angle relative to the +X direction, and clockwise and counter-clockwise rotations were denoted as positive (+) and negative (−), respectively. Figs. 3(d) and 3(e) show that each pad-eye is attached to the specimens and a mooring line was linked to the pad-eye.

2.3 Model Soil and Test Procedure

The soil in which the model suction piles were embedded was prepared using Jumunjin sand with a specific gravity of 2.62 and an internal friction angle of 37.8°. This sand has uniform characteristics and has been frequently used as standardized sand in Korea and can be collected in an area of the East Sea located on the right side of the Korean Peninsula. The detailed material properties and the particle size distribution of Jumunjin sand are listed in Table 2. The relative density of the soil was constituted to D_r = 76.0%.

3. Finite Element Model

3.1 Geometry and Meshes

A three-dimensional finite element (FE) model was developed using the commercial software, ABAQUS/Standard 6.11. The suction pile was represented as an undeformable rigid body with an outside diameter D = 3.0 m, a height L_0 = 6.0 m, and a pile's thickness t = 0.1 m. These dimensions were selected to reflect the prototype dimension of the model suction pile used as the basis for the centrifugal model specimen (see Table 1). The diameter and depth of the soil model were constituted to 10*D* (= 30 m) and 6*D* (= 18 m), respectively. A semi-cylindrical model geometry was applied to reduce the computation time and improve the calculation efficiency. The soil and suction pile consisted of 5,652 and 368 elements, respectively, and 6,950 and 770 nodes, respectively. Each element comprised 8-node brick points (i.e., C3D8). The model bottom was constrained in the x, y, and z directions, while the side of the model was free to displace in the z-direction. The load used to simulate the pullout behavior of the suction pile was applied at various inclination angles to the x-direction (Fig. 4).

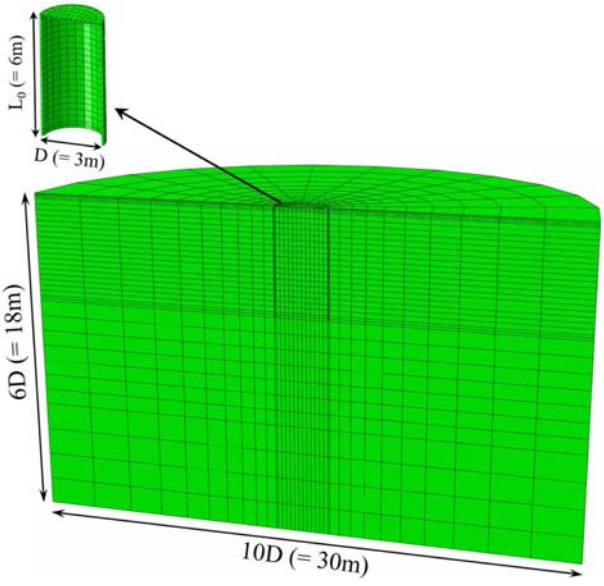

Fig. 4. Axisymmetric Finite Element Mesh for Soil and Suction Pile Models

Table 2. Physical Properties and Particle Size Distribution of Jumunjin Sand

Materials	Value	Particle size distribution curve
Max. dry unit weight (kN/m^3)	16.4	
Min. dry unit weight (kN/m^3)	13.5	
Specific gravity (G_s)	2.62	
Internal friction (˚)	37.8	
D_{10} (mm)	0.44	
Coefficient of uniformity (C_u)	1.20	
Coefficient of curvature (C_g)	0.97	
USCS*	SP	
Poison's ratio	0.30	
Elastic modulus (E, MPa)	26.8	

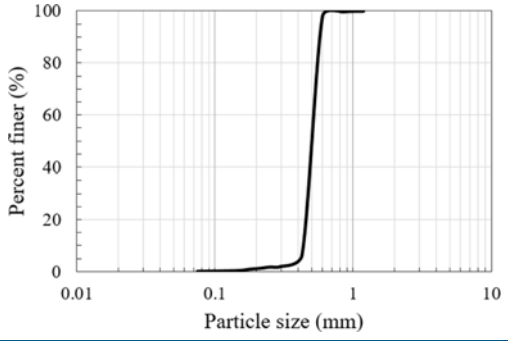

*Abbreviation of the Unified Soil Classification System

3.2 Soil and Interface Properties

The soil was modeled using the Mohr-Coulomb failure criterion with the non-associated flow rule, and a suction pile was simulated based on the isotropic linear-elastic model. In order to simulate the pullout behavior in the numerical analysis, it is necessary to consider the contact surface between the soil and suction pile. In this study, the contact surface between them was modeled by the contact pairs function, which enables the pulled-out simulation of a suction pile from sandy soils, supported by Abaqus 6.11. This function can consider the direction and magnitude of forces and allows that contact-pressure can be propagated between the soil and suction piles as pullout behavior begins. In compliance with this process, we modeled the pullout behavior in this finite element analysis. The soil properties were based on the Jumunjin sand used in the centrifugal model tests. The detailed information related to the input parameters (i.e., unit weight, Poisson's ratio, apparent cohesion (c), friction angle (ϕ), dilation angle (δ), and constant friction angle (μ)), and elastic modulus of suction pile and soil, is shown in Table 3. In the model, the soil was divided into thirty-five layers and the elastic modulus of each layer was determined using Eq. (1) based on the fact that the soil's elastic modulus increases as the confining stress increases with the depth (Duncan and Chang, 1970).

$$E = E_{ref}\left(\frac{p}{p_a}\right)^m, \quad (1)$$

where E_{ref} is the elastic modulus at atmospheric pressure, taken here as 25 MPa, p is the effective stress with depth (kPa), p_a is the atmospheric pressure (= 101.3 kPa), and m is a fitting parameter. In this study, the m value was set to 0.5 according to a comparison of the ultimate pullout capacities obtained from the centrifugal model test and finite element analysis. The resulting elastic modulus profile with depth is shown in Fig. 5.

4. Results and Discussions

4.1 Determination of Ultimate Pullout Capacity

Table 3. Input Parameters of Sand and Suction Pile Model

Parameters		Input
Model criterion	Soil	Mohr-Columb
	Suction pile	Linear-elastic
Unit weight (kN/m^3)	Soil	15.6
	Suction pile	78.0
Poisson's ratio (v)		0.3
Strength parameters (soil)	c (kPa)	0.1
	ϕ (°)	37.8
	δ (°)	7.8
	μ	0.47
Elastic modulus, E	Suction pile	200 GPa
	Soil	See Fig. 5

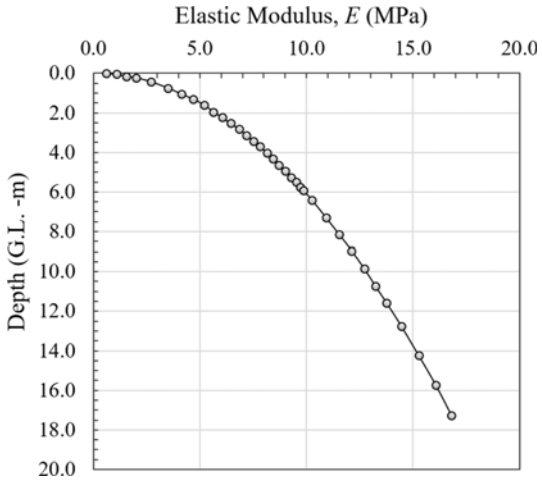

Fig. 5. Elastic Modulus (E) Distribution with the Depth in the FE Model as Determined by Eq. (1)

The model tests were carried out according to the following procedure; 1) after preparing the model soil by placing the sand step-by-step using a sand sifter to achieve a final depth of 22.0 cm (see Fig. 2), the suction pile was installed at 1g using a suction pile installer that was capable of adjusting the suction pile to an accurate location; 2) preliminary centrifuge operation was initiated at 100 g for 5 minutes to stabilize the soil after suction pile installation; 3) the pulling motor was then connected to the embedded suction pile using the pulley system shown in Fig. 2; 4) the initial position of the suction pile was measured in the horizontal and vertical directions from the container wall and top, respectively; 5) the centrifuge was operated for 5 minutes at 100 g while the pullout load was applied to the model suction pile by winding the steel wire on the pulley with a gear; 6) once the measured pullout capacity reached its peak value, the centrifuge was gradually shut down; and 7) the final displacement of the suction pile was measured. The further details of this test procedure were delineated in Jang and Kim (2013). The results plotted in Fig. 6 show the measured pullout resistance depending on various pad-eye positions and inclination angles.

The FE analysis consists of three steps: In Step 1, the initial stress profile in the soil model was generated and allowed to equilibrate using the geostatic option. The space for the installation of the suction pile body was modeled as a void whose boundary was constrained to retain the space for the suction pile. In Step 2, the rigid elements of the suction pile were activated by simulating the installation of the suction pile. The contact behavior was initiated at the interfaces between the suction pile and adjacent soil elements. In which, the surface-to-surface contact function was used to allow gapping and slippage at the boundary between soil and suction pile to simulate the fact that the suction pile was pulled out from the ground. In the final step, the suction pile was loaded at the various pad-eye locations according to the desired inclination angles. The results plotted in Fig. 7 are the calculated pullout resistance with displacement obtained from Step 3.

As shown in Figs. 6 and 7, the pullout resistance-displacement

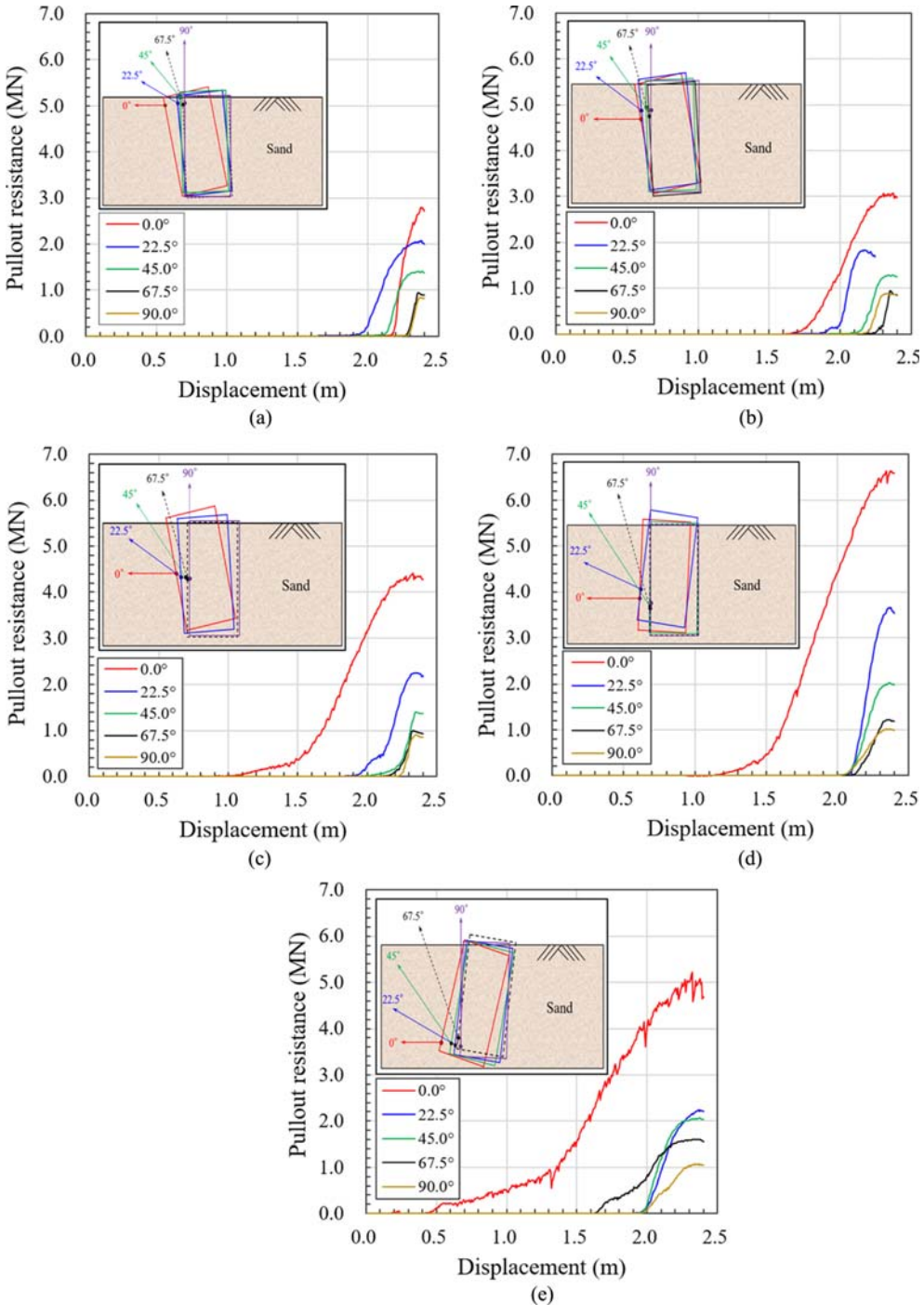

Fig. 6. Pullout Resistance-Displacement Curves and the Rotation Behavior of Suction Piles Obtained from the Centrifugal Model Tests According to the Various Inclination Angles at Pad-Eye Positions: (a) Pad-Eye 5%, (b) Pad-Eye 25%, (c) Pad-Eye 50%, (d) Pad-Eye 75%, (e) Pad-Eye 95%

curves (*hereafter* PR-D curves) obtained from the centrifugal model tests show a peak value clearly while the PR-D curve from the FE analyses continuously increases. This is because the FE analysis was unable to simulate the behavior of the suction pile being fully pulled out. Ahmed and Hawlader (2014) reported that the FE analysis could not secure sufficient displacement to generate the peak value (i.e., ultimate pullout capacity) due to the distortion of meshes. Therefore, it is difficult to determine the ultimate pullout capacity from the PR-D curve of the FE analysis and directly compare it with the ultimate pullout capacity obtained from the centrifugal model test.

In this study, the method described by Villalobos (2006) was applied to define the ultimate pullout capacity of the experimental and FE results, and the determined results were compared directly. In this method, the tangential lines were fitted to the initial stiff elastic section and the plastic section. A horizontal line is then

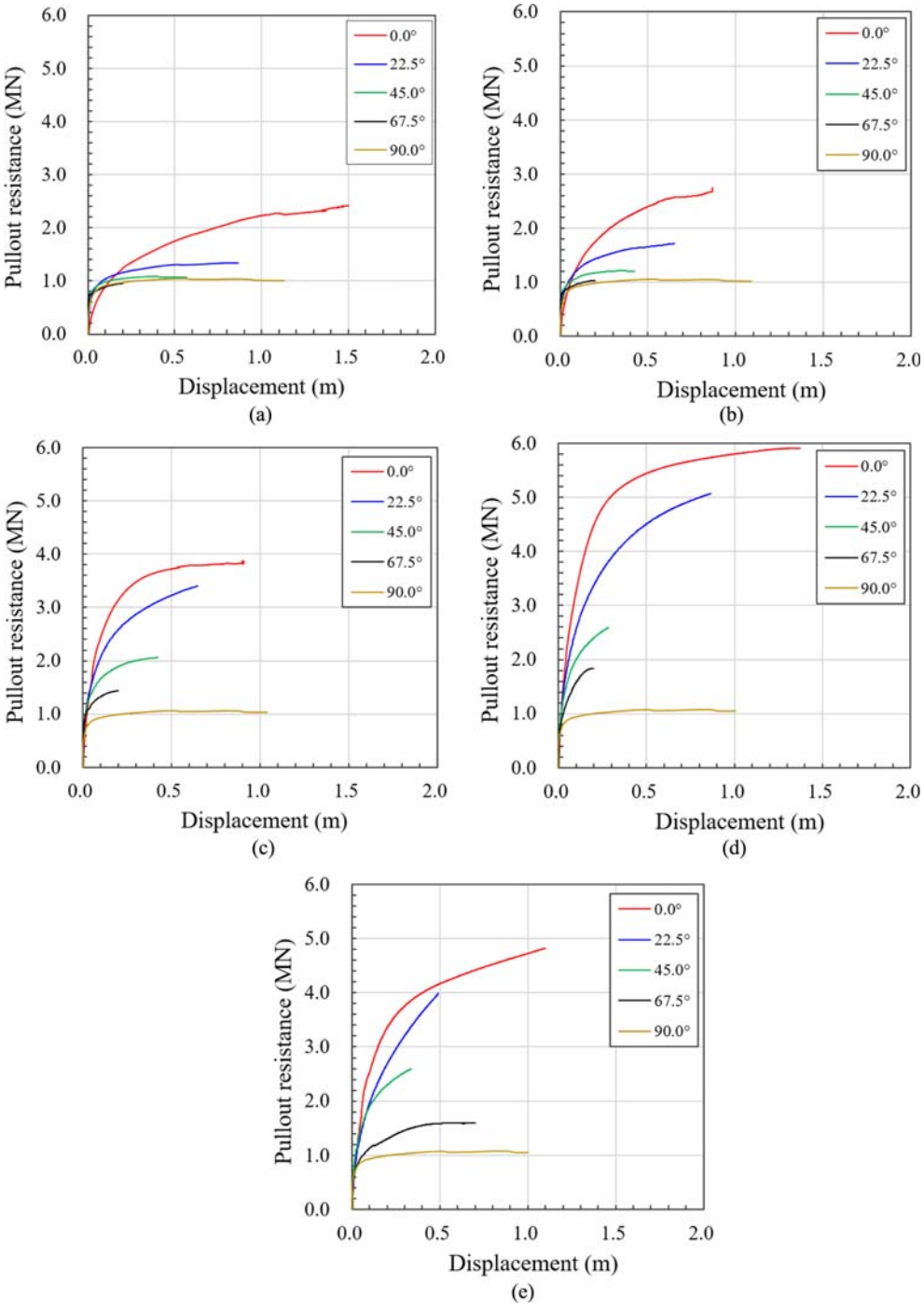

Fig. 7. FE-Determined Pullout Resistance-Displacement Curves According to the Various Inclination Angles at Pad-Eye Positions: (a) Pad-Eye 5%, (b) Pad-Eye 25%, (c) Pad-Eye 50%, (d) Pad-Eye 75%, (e) Pad-Eye 95%

drawn from the intersection point of the two fitted lines to the PR-D curve. This line will be extended until it cuts the PR-D curve, the intersection between the horizontal line and the curve was defined as the ultimate pullout capacity. The ultimate pullout capacity of the centrifugal model test was also determined by applying Villalobos' method to compare with that of the FE analysis. The detailed description is shown in Fig. S2.

4.2 Ultimate Pullout Capacity

The ultimate pullout capacities were determined using Villalobos's method in the PR-D curves obtained from the centrifugal model tests and the FE analyses (See Section 4.1). Each ultimate pullout capacity is shown in Fig. 8.

The ultimate pullout capacity increased as the inclination angle approached zero, and as the pad-eye position approached 75% of the suction pile length below the lid. This means that the

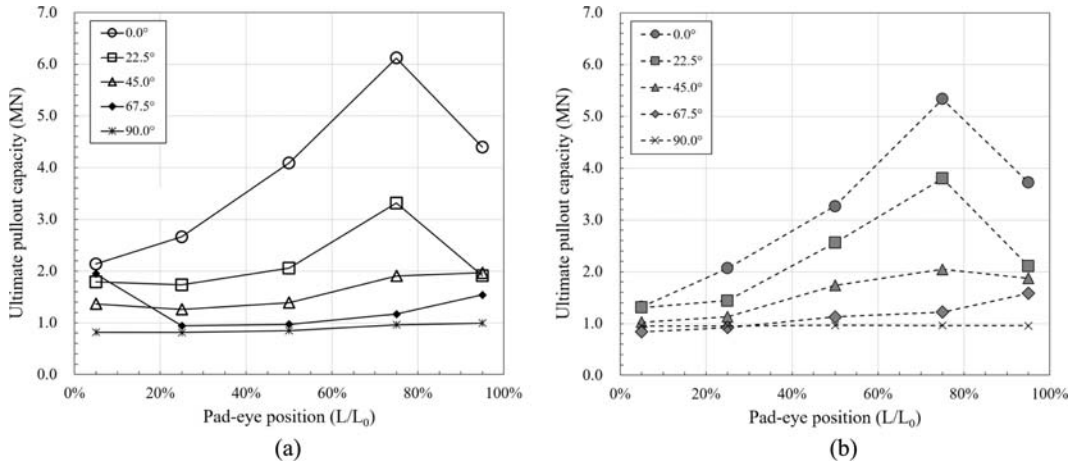

Fig. 8. Ultimate Pullout Capacity Obtained from the Centrifugal Model Test and Finite Element Analysis: (a) Centrifugal Model Test, (b) Finite Element Analysis

inclination angle and pad-eye significantly influence the ultimate pullout capacity. In addition, the reason why the ultimate pullout capacity increases as the inclination angle decreases and the pad-eye position moves to the bottom of the suction pile is that the passive earth pressure increases as well as the increase of friction between soil and suction pile, during pulling out the pile.

4.3 Failure Envelopes

During the operation of offshore facilities, the suction piles used as the foundations are subjected to the combined vertical-horizontal (V-H) loading depending on the inclination angle and the pad-eye position. This loading can be defined as the concept of the failure envelope extended from the ratio of vertical and horizontal load components (i.e., V/V_{ult} and H/H_{ult}). In which, V/V_{max} and H/H_{max} are the ratios of the vertical and horizontal load components and the ultimate vertical and horizontal pullout capacities, respectively (Bransby and Randolph, 1999; Deng and Carter, 2000; Cho and Bang, 2002; Supachawarote et al., 2004; Bang et al., 2011).

The failure envelope for suction piles has typically been determined through the physical model test (Byrne and Houlsby, 2004; Kelly et al., 2006; Zhan and Liu, 2010; Ibsen et al., 2014), numerical analysis (Bransby and Randolph, 1998; Geourvenec and Randolph, 2003; Supachawarote et al., 2004; Zhan and Liu, 2010; Ahn et al., 2014; Liu et al., 2014; Zou et al., 2018; Zhao et al., 2019; KNOC, 2023), and the limit state analysis based on the plastic theory (Randolph et al., 1998; Deng and Carter, 2000; Aubeny et al., 2003; Faizi et al., 2020). In this study, the failure envelopes for the various pad-eye positions were determined using the results of the centrifugal model tests and FE analyses by changing the inclination angles.

The vertical and horizontal load components, obtained from the centrifugal model tests and FE analyses, are plotted in Fig. 9. These curves were expressed in the form of quadratic equations to inform the determination of the failure envelopes. Since the ultimate pullout capacities associated with the pad-eye positions 5% and 25% were much smaller than those values related to the pad-eye position 50% (See Fig. 8), the failure envelopes related to the pad-eye positions 5% and 25% are not presented in Fig. 9. These failure envelopes can be approximated as Eq. (2). In addition, the shape of the failure envelopes seems like an upward convex-shape. Deng and Carter (2000), who initially analyzed the pullout behavior of suction piles embedded in sandy soil, also reported that the failure envelope for suction piles embedded in sandy soil was upward convex-shape. The factors (i.e., a and b) were determined by the method of least squares and are shown in Table 4.

$$\left(\frac{V}{V_{ult}}\right) = 1 + a\left(\frac{H}{H_{ult}}\right) + b\left(\frac{H}{H_{ult}}\right)^2, \tag{2}$$

where V and H are the vertical and horizontal components of pullout capacity, V_{ult} and H_{ult} are the ultimate vertical and horizontal

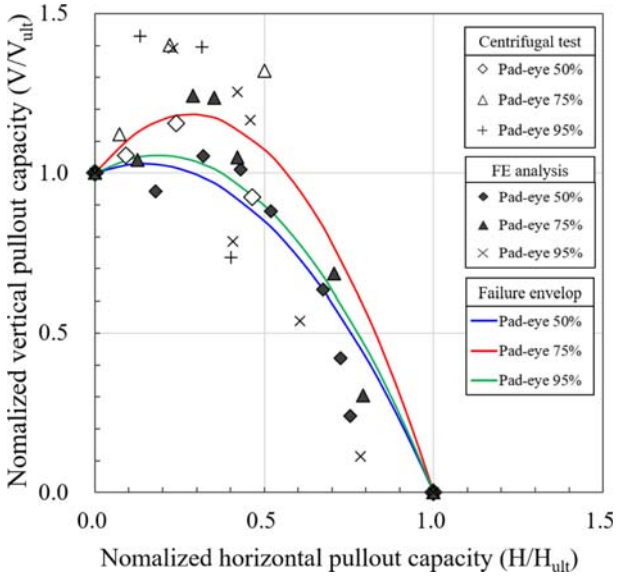

Fig. 9. Failure Envelopes Suggested in This Study according to the Pad-eye Positions

Table 4. The Factors for Each Pad-Eye Position, Related to Eq. (2)

Factors	Pad-eye position (%)		
	50	75	95
a	0.4	1.3	0.6
b	-1.4	-2.3	-1.6

pullout capacities, *a* and *b* are the functions of normalized the length and diameter of the suction pile, and are expressed as $a = 0.5 + L/D$ and $b = 4.5 - L/3D$. The L and D are the length and diameter of the suction pile.

4.4 Practical Implication for Mooring System

In general, the catenary and taut-leg mooring systems are used to connect the suction piles to the floating structure, and these mooring systems employ inclination angles ranging from 10° to 15° and from 30° to 40° to the horizontal, respectively (Tjelta, 2001). As far as the foregoing description, the inclination angles for each mooring are pre-determined. Therefore, the pad-eye position is a notable factor for mooring systems in the given inclination angles. In this section, the optimal pad-eye positions for the catenary and taut-leg mooring system were investigated to obtain the largest ultimate pullout capacity and minimize the rotation of the suction pile.

The ultimate pullout capacities and rotation angles with the pad-eye position are shown in Fig. 10 for each mooring system, based on the additional FE analyses. For the catenary mooring system, the largest ultimate pullout capacity was generated when the pad-eye was located at 75% of the suction pile length below the lid. The suction pile was pulled out without rotation when the pad-eye was located at approximately 70% of the suction pile length (Fig. 10(a)). Similarly, for the taut-leg mooring system, the largest ultimate pullout capacity was obtained when the pad-eye was located at 75% of the pile length below the top. The rotation of the suction pile was close to 0° when the pad-eye position was located at 65% of the pile length (Fig. 10(b)).

Based on these results, the ultimate pullout capacity of the catenary mooring system was evaluated to be about 1.94 times that of the taut-leg mooring system under the same condition (i.e., pad-eye was located at 75% of the suction pile length below the lid). Therefore, it can be considered that the catenary mooring system is a better option for mooring offshore facilities than the taut-leg mooring system. However, since the length of the mooring line for the catenary mooring system is typically longer than that for the taut-leg mooring system, the appropriate mooring system should be determined based on the type of offshore facility required.

In addition, recently, construction companies in Korea, that are planning to build offshore wind turbines on saturated sand, decided that suction piles will be used for the mooring system (KNOC, 2023). We believe that the results of this study will be sufficient indicators and basis for engineers who will analyze the pullout behavior of suction piles in order to secure the safety of offshore wind turbines.

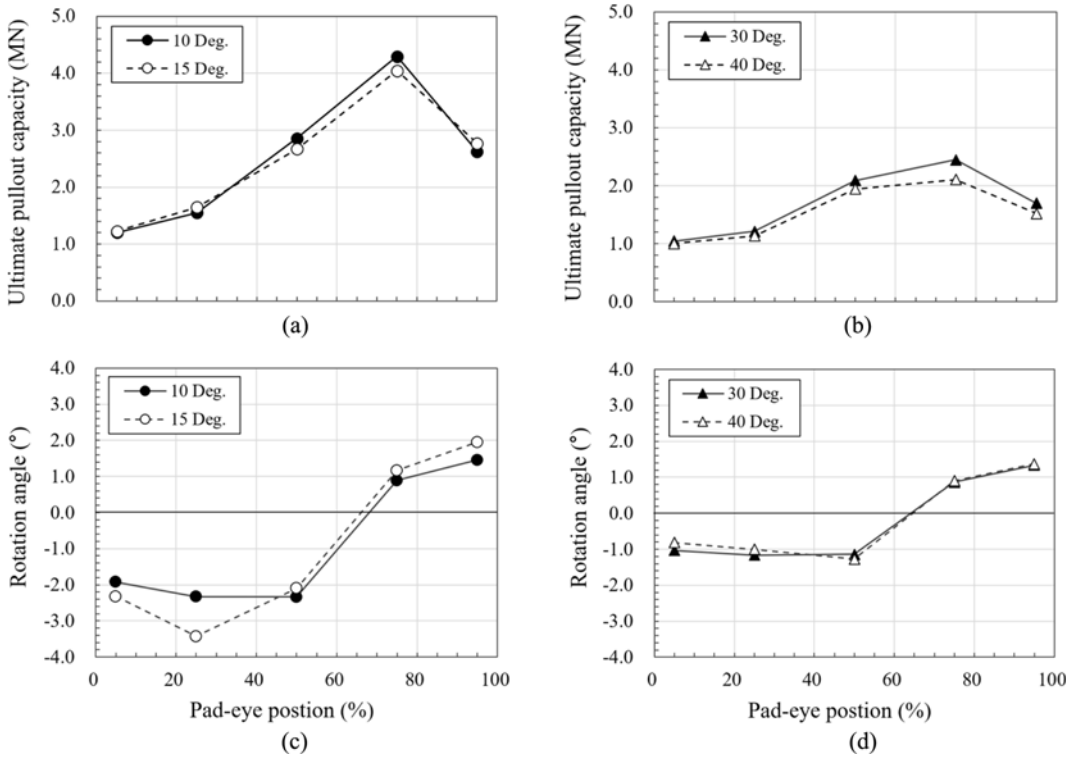

Fig. 10. Changes in the Ultimate Pullout Capacities and Rotation Angles with the Pad-Eye Positions: (a) Catenary Mooring, (b) Taut-Leg Mooring

5. Conclusions

In this study, centrifugal model tests and finite element analyses were carried out to investigate the pullout behavior of the suction pile embedded in saturated sand according to various inclination angles and pad-eye positions. The centrifugal model tests of suction pile models embedded in Jumunjin sand were operated at 100 g level. The FE model adopted the Mohr-Coulomb failure criterion with the non-associated flow rule. The pullout resistance-displacement curves obtained from the centrifugal model tests and FE analyses were used to determine the ultimate pullout capacities for each inclination angle and pad-eye position using Villalobos' method. The following conclusions are drawn from the analysis results.

The ultimate pullout capacity was observed to increase as the inclination angle approached zero degree and as the pad-eye position approached 75% of the suction pile length below the lid. This means that the inclination angle and pad-eye significantly influence the ultimate pullout capacity. In addition, the reason why the ultimate pullout capacity increases as the inclination angle decreases and the pad-eye position moves to the bottom of the suction pile, is that the passive earth pressure increases as well as the increase of friction between soil and suction pile.

Based on the determined ultimate pullout capacities, the vertical-horizontal failure envelopes were proposed for pad-eye positions ranging from 50% to 95% to provide an improved method for the rational design of offshore foundations in the coastal environment.

In addition, the optimal pad-eye positions for the catenary and taut-leg mooring systems, which are widely used as foundations for floating structures, were investigated by performing additional FE analyses. For both mooring systems, the largest ultimate pullout capacity was generated when the pad-eye was located at 75% of the suction pile length below the lid. Based on the result, the ultimate pullout capacity of the catenary mooring system was evaluated to be approximately 1.94 times that of the taut-leg mooring system under the same condition.

Acknowledgments

Not Applicable

ORCID

Not Applicable

References

Ahmed SS, Hawlader BC (2014) Finite element modeling of inclined load capacity of suction caisson in sand with Abaqus/Explicit. Proc the Twenty-fourth Int Ocean Polar Eng, Busan, Korea, 463-469

Ahmed SS, Hawlader BC (2015) Numerical analysis of inclined uplift capacity of suction caisson in sand. *International Journal of Offshore and Polar Engineering* 25(2):145-155, DOI: 10.17736/ijope.2015.cg11

Ahn J, Lee H, Kim YT (2014) Finite element analysis of the holding capacity of shallow suction caisson anchors. *Marine Georesources & Geotechnology* 33(1):33-44, DOI: 10.1080/1064119X.2013.778377

Andersen KH, Jostad HP (1999) Foundation design of skirted foundations and anchors in clay. In Offshore Technology Conference, Houston, Texas, USA, DOI: 10.4043/10824-MS

Aubeny CP, Han SW, Murf JD (2003) Inclined load capacity of suction caissons. *International Journal for Numerical and Analytical Methods in Geomechanics* 27(14):1235-1254, DOI: 10.1002/nag.319

Bang S, Jones KD, Kim KO, Kim YS, Cho Y (2011) Inclined loading capacity of suction piles in sand. *Ocean Engineering* 38(7):915-924, DOI: 10.1016/j.oceaneng.2010.10.019

Bransby M, Randolph M (1998) Combined loading of skirted foundations. *Géotechnique* 48(5):637-655, DOI: 10.1680/geot.1998.48.5.637

Bransby MF, Randolph M (1999) The effect of embedment depth on the undrained response of skirted foundations to combined loading. *Soils and Foundations* 39(4):19-33, DOI: 10.3208/sandf.39.4_19

Byrne BW, Houlsby GT (2004) Experimental investigation of the cyclic response of suction caisson in sand. International Offshore Technology Conference, Houston, Texas, USA, OTC 12194, DOI: 10.4043/12194-MS

Cho Y, Bang S (2002) Inclined loading capacity of suction piles. In The Twelfth International Offshore and Polar Engineering Conference, Kitakyushu, Japan, 827-832

Deng W, Carter JP (2000) Inclined uplift capacity of suction caissons in sand. International Offshore Technology Conference, Houston, Texas, USA, OTC-12196, DOI: 10.4043/12196-MS

Duncan JM, Chang CY (1970) Nonlinear analysis of stress and strain in soils. *Journal of the Soil Mechanics and Foundations Division* ASCE 96(5):1629-1653, DOI: 10.1061/JSFEAQ.0001458

Faizi K, Faramarzi A, Dirar S, Chapman D (2020) Development of an analytical model for predicting the lateral bearing capacity of caisson foundations in cohesionless soils. *Ocean Engineering* 218: 1-13, DOI: 10.1016/j.oceaneng.2020.108112

Gao Y, Qiu Y, Li B, Li D, Sha C, Zheng X (2013) Experimental studies on the anti-uplift behavior of the suction caissons in sand. *Applied Ocean Research* 43:37-45, DOI: 10.1016/j.apor.2013.08.001

Geourvenec S, Randolph M (2003) Effect of strength non-homogeneity on the shape of failure envelopes for combined loading of strip and circular foundations on clay. *Géotechnique* 53(6):575-586, DOI: 10.1680/geot.2003.53.6.575

Ibsen LB, Larsen KA, Barari A (2014) Calibration of failure criteria for bucket foundations on drained sand under general loading. *Journal of Geotechnical and Geoenvironmental Engineering* 140(7):1-16, DOI: 10.1061/(ASCE)GT.1943-5606.0000995

Jang YS, Kim YS (2013) Centrifugal model behavior of laterally loaded suction pile in sand. *KSCE Journal of Civil Engineering* 17(5):980-988, DOI: 10.1007/s12205-013-0011-z

Keawsawasvong S, Yoonirundorn K, Senjuntichai T (2021) Pullout capacity factor for cylindrical suction caissons in anisotropic clays based on anisotropic undrained shear failure criterion. *Transportation Infrastructure Geotechnology* 8:629-644, DOI: 10.1007/s40515-021-00154-x

Kelly RB, Houlsby GT, Byrne BW (2006) A comparison of field and laboratory tests of caisson foundations in sand and clay. *Géotechnique* 56(9):617-626, DOI: 10.1680/geot.2006.56.9.617

Kim S, Choo YW, Kim DS (2016) Pullout capacity of horizontally loaded suction anchor installed in silty sand. *Marine Georesources & Geotecnology* 34(1):87-95, DOI: 10.1080/1064119X.2014.961622

Kim S, Choo YW, Kim JH, Kim DS, Kwon O (2015) Pullout resistance of group suction anchors in parallel array installed in silty sand

subjected to horizontal loading - Centrifuge and numerical modeling. *Ocean Engineering* 107:85-96, DOI: 10.1016/j.oceaneng.2015.07.037

Kim YS (2014) A study of pullout behavior of a suction pile in sandy soils by centrifugal model test. PhD Thesis. Dongguk University, Seoul, South Korea (in Korean)

KNOC (2023) Floating offshore wind farm projects. Korea National Oil Corporation, Retrieved March 3, 2023, https://www.knoc.co.kr/ENG/sub03/sub03_9_2.jsp

Koh KX, Hossain MS, Kim Y (2017) Installation and monotonic pullout of a suction caisson anchor in calcareous silt. *Journal of Geotechnical and Geoenvironmental Engineering* 143(2):1-13, DOI: 10.1061/(ASCE)GT.1943-5606.0001604

Lee S, Tran NX, Kim SR (2017) Experimental investigation of the vertical pullout cyclic response of bucket foundations in sand, *Applied Ocean Research* 68:325-335, DOI: 10.1016/j.apor.2017.06.006

Li Z, Kotronis P, Escoffier S (2014) Numerical study of the 3D failure envelope of a single pile in sand. *Computers and Geotechnics* 62: 11-26, DOI: 10.1016/j.compgeo.2014.06.004

Liu M, Yang M, Wang H (2014) Bearing behavior of wide-shallow bucket foundation for offshore wind turbines in drained silty sand. *Ocean Engineering* 82:169-179, DOI: 10.1016/j.oceaneng.2014.02.034

Petel SK, Singh B (2019) A parametric study on the vertical pullout capacity of suction caisson foundation in cohesive soil. *Innovative Infrastructure Solutions* 4(1):1-11, DOI: 10.1007/s41062-018-0188-6

Randolph M, Houlsby GT (1984) The limiting pressure on a circular pile loaded laterally in cohesive soil. *Géotechnique* 34(4):613-623, DOI: 10.1680/geot.1984.34.4.613

Randolph M, House AR (2002) Analysis of suction caisson capacity in clay. International Offshore Technology Conference, Houston, Texas, USA, DOI: 10.4043/14236-MS

Randolph M, O'Neill M, Stewart D (1998) Performance of suction anchors in fine-grained calcareous soils. International Offshore Technology Conference, 521-529, DOI: 10.4043/8831-MS

Ssenyondo V, Hong S, Bong T, Kim SR (2021) Effect of embedment depth on the pullout capacity of bucket foundations in sand. *Ocean Engineering* 237:1-13, DOI: 10.1016/j.oceaneng.2021.109643

Supachawarote C, Randolph M, Gourvenec S (2004) Inclined pullout capacity of suction caissons. The 14th International Offshore Polar Engineering Conference, Toulon, France, ISOPE-I-04-238

Tjelta TI (2001) Suction piles: Their position and application today. T*he 11th International Offshore Polar Engineering Conference, Stavanger, Norway* 2:1-6

Villalobos J (2006) Model testing of foundations for offshore wind turbines. PhD Thesis, University of Oxford, England (in English)

Zhan Y, Liu F (2010) Numerical analysis of bearing capacity of suction bucket foundation for offshore wind turbines. *Electronic Journal of Geotechnical Engineering* 15(10):76-81

Zhao L, Bransby MF, Gaudin C (2020) Centrifuge observations on multidirectional loading of a suction caisson in dense sand. *Acta Geotechnica* 15:1439-1451, DOI: 10.1007/s11440-020-00970-4

Zhao L, Gaudin C, O'Loughlin CD, Hambleton JP, Cassidy MJ, Herduin M (2019) Drained capacity of a suction caisson in sand under inclined loading. *Journal of Geotechnical and Geoenvironmental Engineering* 145(2):1-12, DOI: 10.1061/(ASCE)GT.1943-5606.0001996

Zou X, Hu Y, Hossain MS, Zhou M (2018) Capacity of skirted foundations in sand-over-clay under combined V-H-M loading. *Ocean Engineering* 159:201-218, DOI: 10.1016/j.oceaneng.2018.04.007